

Less is More: Learning from Synthetic Data with Fine-grained Attributes for Person Re-Identification

Suncheng Xiang¹, Guanjie You², Mengyuan Guan¹, Hao Chen¹, Binjie Yan¹, Ting Liu¹, Yuzhuo Fu¹
¹Shanghai Jiao Tong University, ²National University of Defense Technology

{xiangsuncheng17, gemini.my, 958577057, yanbinjie, lousia_liu, yzfu}@sjtu.edu.cn, ygjssxz@163.com



Figure 1. Sample images from the proposed *FineGPR* dataset, which contains 2,028,600 images of 1,150 identities. We manually labeled fine-grained attribute annotations both at environment level and identity level. *First row*: With the same characters in different scenes, in each scene, a person can face toward a manually denoted direction. *Second row*: Different characters in the same scene (*i.e.* Scene #6).

Abstract

*Person re-identification (re-ID) plays an important role in applications such as public security and video surveillance. Recently, learning from synthetic data, which benefits from the popularity of synthetic data engine, has attracted great attention from the public eyes. However, existing datasets are limited in quantity, diversity and realism, and cannot be efficiently used for re-ID problem. To address this challenge, we manually construct a large-scale person dataset named FineGPR with fine-grained attribute annotations. Moreover, aiming to fully exploit the potential of FineGPR and promote the efficient training from millions of synthetic data, we propose an attribute analysis pipeline called AOST, which dynamically learns attribute distribution in real domain, then eliminates the gap between synthetic and real-world data and thus is freely deployed to new scenarios. Experiments conducted on benchmarks demonstrate that FineGPR with AOST outperforms (or is on par with) existing real and synthetic datasets, which suggests its feasibility for re-ID task and proves the proverbial **less-is-more** principle. Our synthetic FineGPR dataset is publicly available at <https://github.com/JeremyXSC/FineGPR>.*

1. Introduction

Given a query image, person re-identification aims to match images of the same person across non-overlapping camera views, which has attracted lots of interests and attention in both academia and industry. Encouraged by the remarkable success of deep learning networks [16, 26] and the availability of re-ID datasets [28, 46], performance of person re-ID has been significantly boosted and made great progress. However, in practice, manually labelling a large diversity of training data is time-consuming and labor-intensive when directly deploying re-ID system to new scenarios. During intensive annotation, one needs to associate a pedestrian across different cameras, which is a difficult and laborious process as people might exhibit very different appearances in different cameras. In addition, there also has been an increasing concern over data safety and ethical issues, *e.g.* DukeMTMC-reID [28, 47] has been taken down due to privacy problem. Some European countries already passed privacy-protecting laws [13] to prohibit the acquisition of personal data without authorization, which makes collection of large-scale datasets extremely difficult.

To address this challenge, several works [1, 2, 32, 38] have proposed to employ off-the-shelf game engines to generate synthetic person images. For example, Barbosa *et al.* [2]

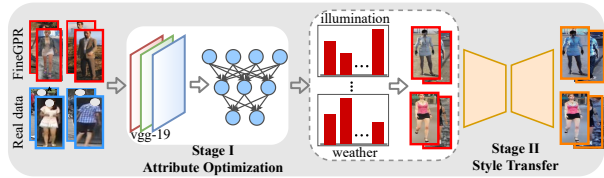


Figure 2. System workflow of the AOST method, which is based on the dataset with fine-grained attribute annotations.

construct a SOMAset which contains 50 3D human models. SyRI [1] provides 100 virtual humans rendered with 140 HDR environment maps. Wang *et al.* [38] collect a Rand-Person dataset with 1,801,816 synthesized person images. Although these datasets provide considerable benefits of the data scale and enable some preliminary research in person re-ID, they are quite limited in both the attribute distribution and collected environment, *e.g.*, SyRI does not have concept of cameras, and SOMAset is uniformly distributed along an environment with clothing variations. In essence, these synthetic datasets either focus on independent attribute, or require annotators to carefully simulate specific scenes in detail, few datasets consider fine-grained attribute annotations or high-quality image resolution, which limits their scalability and diversity in terms of synthesized person. Another challenge we could observe is that, previous methods mainly focus on achieving competitive performance with large-scale data at the sacrifice of expensive time costs and intensive human labors, while neglect to perform efficient training with a higher quality of attribute annotations from millions of synthetic data. Considering the fact that existing real-world datasets can be very different in terms of content and style, *e.g.*, Market-1501 [46] consists mostly of summer scenes captured in campus, while light in the CUHK03 [21] covers a wide range of indoor scenes, directly using all synthetic dataset for training will undoubtedly produce negative effects for domain adaptation, which makes it infeasible in practical scenarios.

In order to alleviate the problems identified above and facilitate the study of re-ID community, we start from two perspectives, namely data and methodology. From the aspect of the data, we propose to collect data from synthetic world on the basis of GTA5 game engine, and manually construct a **Fine**-grained **GTA Person Re-ID** dataset called *FineGPR*, which provides accurate and configurable annotations, *e.g.*, *viewpoint, weather, diverse and informative illumination and background*, as well as the various *pedestrian attribute annotations at the identity level*. Compared to existing person re-ID datasets, *FineGPR* is explicitly distinguished in richness, quality and diversity. It is worth noting that our data synthesis engine is still extendable to generate more data, which can be edited/extended not only for this study, but also for future research in re-ID community.

From the aspect of methodology, we introduce a novel **Attribute Optimization and Style Transfer** pipeline **AOST** to perform training on re-ID task in a data-efficient manner. AOST can dynamically select samples which approximates the attribute distribution in real domain. As illustrated in Fig. 2, the proposed AOST contains Stage-I (*Attribute Optimization*) and Stage-II (*Style Transfer*). Firstly, Stage-I is adopted to mine the attribute distribution of real domain, following by the Stage-II to reduce the intrinsic gap between synthetic and real domain. Finally, the transferred data are adopted for performing training on downstream vision task. This is the first time as far as we know, to greatly promote efficient training from millions of synthetic data on re-ID task, experiments across diverse datasets suggest that the “*less-is-more*” principle is highly effective in practice.

Our contributions can be summarized into three aspects:

- We open source the largest person dataset with fine-grained attribute annotations for the community without privacy and ethics concerns.
- Based on it, we propose a two-stage pipeline AOST to learn from fine-grained attributes, then eliminate style differences between synthetic and real domain for more efficient training.
- Extensive experiments conducted on benchmarks show that our *FineGPR* is promising and can achieve competitive performance with AOST in re-ID task.

2. Related Works

2.1. Person re-ID Methods

In the field of person re-ID, early works [23, 45] either concentrate on hand-crafted feature or low-level semantic feature. Unfortunately, these methods always fail to produce competitive results because of their limited discriminative learning ability. Recently, benefited from the advances of deep neural networks, person re-ID performance in supervised learning has been significantly boosted to a new level [5, 22, 36], which learned robust feature extraction and reliable metric learning in an end-to-end manner. Typically, person re-ID model can be trained with the identification loss [41], contrastive loss [34, 35] and triplet loss [17]. Recently, a strong baseline [25] for re-ID is employed to extract the discriminative feature, which has been proved to have great potential to learn a robust and discriminative model in person re-ID models. Besides, several literatures [9, 40] focus on the image-level to allow different domains to have similar feature distributions, or adopt an adversarial domain adaptation approach to mitigate the distribution shift [11, 33], which has attracted considerable attention from various fields in re-ID community.

Dataset		#Identities	#Bboxes	#Cameras	#Wea.	#Illum.	#Scenes	#ID-level	#Resolution	Hard samples	Ethical Considerations
Real	Market-1501 [46]	1,501	32,668	6	×	×	×	✓	low	No	No
	CUHK03 [21]	1,467	14,096	2	×	×	×	×	low	No	No
	MSMT17 [39]	4,101	126,441	15	×	×	×	×	vary	No	No
Synthetic	SOMAsSet [2]	50	100,000	250	×	×	×	×	–	No	No
	SyRI [1]	100	1,680,000	280	×	140	×	×	–	No	No
	PersonX [32]	1,266	273,456	6	×	×	3	×	vary	No	No
	Unreal [43]	3,000	120,000	34	×	×	4	×	low	Many	No
	RandPerson [38]	8,000	1,801,816	19	×	×	11	×	low	No	No
<i>FineGPR (Ours)</i>		1,150	2,028,600	36	7	7	9	✓	high	Many	Addressed

Table 1. Comparison of some real-world and synthetic person re-ID datasets. In particular, “#Wea.”, “#Illum.”, “#Scenes” and “ID-level” indicate whether dataset has human-annotated labels in terms of weather, illumination, background and ID-level attributes, respectively.

2.2. Person re-ID Datasets

Being the foundation of more sophisticated re-ID techniques, the pursuit of better datasets never stops in the area of person re-ID. Early attempts could be traced back to VIPeR [15], ETHZ [30] and RAiD [7]. More challenging datasets are proposed subsequently, including Market-1501 [46], CUHK03 [21], MSMT17 [39], *etc.* However, labelling such a large-scale real-world dataset is labor-intensive and time-consuming, sometimes there even exists security and privacy problems. Besides, all of these datasets only have limited attribute distribution and are lack of diversity. As the performance gain is gradually saturated on the above datasets, newly large-scale datasets are needed urgently to further boost re-ID performance. Recently, leveraging synthetic data is an effective idea to alleviate the reliance on large-scale real-world datasets. This strategy has been applied in various computer vision tasks, *e.g.*, object detection [27], crowd counting [37] and semantic segmentation [6]. In the person re-ID community, many re-ID methods [1, 2, 32, 38] have proposed to take advantage of game engine to construct large-scale synthetic re-ID datasets, which can be used to pre-train or fine-tune CNN network. For example, Barbosa *et al.* [2] propose a synthetic dataset SOMAsSet created by photo-realistic human body generation software to enrich the diversity. Recently, Wang *et al.* [38] collect a virtual dataset RandPerson with 3D characters containing 1,801,816 synthetic images of 8,000 identities. However, these datasets are either in a small scale or lack of diversity, few of them provide rich attribute annotations, which cannot satisfy the need of attribute learning in person re-ID task. So new fine-grained annotated datasets are urgently needed.

3. The *FineGPR* Dataset

In this section, we describe *FineGPR*, a new dataset with high-quality annotations and multiple attribute distributions to re-ID community. Below we at first review the process of constructing and annotation collection, then present an analysis over dataset statistics. We show some sample images from the proposed *FineGPR* dataset in Fig. 1.

3.1. Dataset Collection

Our *FineGPR* dataset is collected from a popular game engine called the Grand Theft Auto V (GTA5). Practically, we create a synthetic controllable world containing 2,028,600 synthesized person images of 1,150 identities. Images in this dataset generally contain different attributes in a large scope, *e.g.*, **Viewpoint**, **Weather**, **Illumination**, **Background** and **ID-level annotations**, also including many hard samples with occlusion. It is worth noting that, all images are simultaneously captured by 36 non-overlapping cameras with a high resolution and image quality. In the process of image generation, each person walks along a schedule route, and cameras are set up and fixed at the chosen locations. As a controllable system, it can satisfy various data requirements in a fine-grained fashion.

3.2. Properties of *FineGPR* dataset

The goal of our *FineGPR* dataset is to introduce a new challenging benchmark with high-quality annotations and multiple attribute distribution to re-ID community. To the best of our knowledge, this is the first large-scale person dataset with over 4 environment-level attributes and 13 ID-level attribute annotations.

Identities. According to the Table 1, *FineGPR* contains 1,150 hand-crafted identities including females and males, with resolution of 200×480 . To ensure diversity, we cropped human region with different angles. As shown in Fig. 1 (*second row*), different person has different body shape, clothing, hairstyle, and the motion can be randomly set as walking, running, standing and so on. Particularly, the clothes of these characters include jeans, pants, shorts, skirts, T-shirts, dress shirts, *etc.*, and some of these identities have a backpack, shoulder bag, and wear glasses or hat. In total, we manually annotate the *FineGPR* with 13 different pedestrian attributes at the identity level (*e.g.*, wearing dress or not), the distribution diagram is demonstrated in Fig. 3.

Viewpoint. We construct the image exemplars under specified viewpoints. Those images are randomly sampled during normal walking, running, *etc.* Formally, a person image is sampled every 10° from 0° to 350° . (36 different



Figure 3. The distributions of attributes at the identity level on *FineGPR*. The left figure shows the numbers of IDs and category cloud for each attribute. The middle and right pies illustrate the distribution of the colors of upper-body and low-body clothes respectively.

types of viewpoints in total). There are 49 images for each viewpoint of an identity in the entire *FineGPR*, so each person has 1,764 (49×36) images in total.

Weather. Currently, the proposed *FineGPR* has 7 different weather conditions, including Sunny, Clouds, Overcast, Foggy, Neutral, Blizzard and Snowlight. It is worth mentioning that the number of instances in each weather condition is the same, but not a natural heavy-tail distribution, which makes it adaptable to various real-world scenarios.

Illumination. Illumination is another critical factor that contributes to the success of generalizable re-ID, which consists of 7 different types of illumination, *e.g.* midnight (time period during 23:00–4:00 in 24 hours a day.), dawn (4:00–6:00), forenoon (6:00–11:00), noon (11:00–13:00), afternoon (13:00–18:00), dusk(18:00–20:00) and night (20:00–23:00). Parameters like time setting can be modified manually for each illumination type. By editing the values of these terms, various kinds of illumination environments can be created.

Background. GTA5 has a very large environment map, including thousands of realistic urban areas and wild scenes. From now, 9 different scenes are selected to represent real-world scenarios with annotations, *e.g.* street, mall, school, park and mountain, *etc.*, which are distributed evenly across all identities. The different scenes are shown in Fig. 1 (*first row*). More additional details related to our *FineGPR* can be found in the Supplementary Material.

Ethical Considerations. People-centric datasets pose some challenges of data privacy [10] and intersectional accuracy disparities [3]. To address such concerns, our dataset were created with careful attention to ethical questions, which we encountered throughout our work. Access to our dataset will be provided for research purposes only and with restrictions on redistribution. Furthermore, we are very cautious of annotation procedure of *FineGPR* dataset to avoid the social and ethical implications. As for re-ID system, governments and officials must establish strict regulations to control the usage of this technology since it mainly relies on (not all) surveillance data. Motivated by this, we do not

consider the dataset for developing non-research systems unless further professional processing or augmentation.

4. Methodology of Proposed AOST

In this section, we design an effective training strategy AOST to directly select samples on the basis of synthetic *FineGPR* for initializing the re-ID backbone. And the overall framework is illustrated in Fig. 4, which includes two stages: Attribute Optimization and Style Transfer.

Attribute Optimization. Intuitively, since *FineGPR* is a large-attribute-range dataset, using entire *FineGPR* for training is time-consuming and low-efficient. To further exploit the potential of *FineGPR* and promote the training efficiency, we introduce a novel strategy to learn some representative attributes with prior target knowledge. Following the procedure in [12], we adopt a widely used backbone VGG-19 [31] pre-trained on ImageNet [8] to obtain the style distance $\mathcal{D}_{\text{style}}$ and content distance $\mathcal{D}_{\text{content}}$ respectively, which are formulated as:

$$\mathcal{D}_{\text{content}} = \frac{1}{2} \sum_{i,j} (F_{ij}^l - P_{ij}^l)^2 \quad (1)$$

$$\mathcal{D}_{\text{style}} = \sum_{l=0}^L w_l \frac{1}{4N_l^2 M_l^2} \sum_{i,j} (G_{ij}^l - A_{ij}^l)^2 \quad (2)$$

where F_{ij}^l and P_{ij}^l denote representations extracted by the i^{th} filter at position j in layer l of VGG-19. w_l is a hyper-parameter which controls the importance of each layer to the style. N_l represents the number of filters and M_l is size of the feature map. G_{ij} and A_{ij} denote the Gram Matrix of real and synthetic images in layer l . Then total distance for attribute metric is represented as

$$\mathcal{D}_{\text{total}} = \alpha * \mathcal{D}_{\text{style}} + \beta * \mathcal{D}_{\text{content}} \quad (3)$$

where α and β are two hyper-parameters which control the relative importance of style and content distance respectively. As depicted in Algorithm 1, a tree boosting system named XGBoost [4] model θ_0 is trained with *FineGPR*

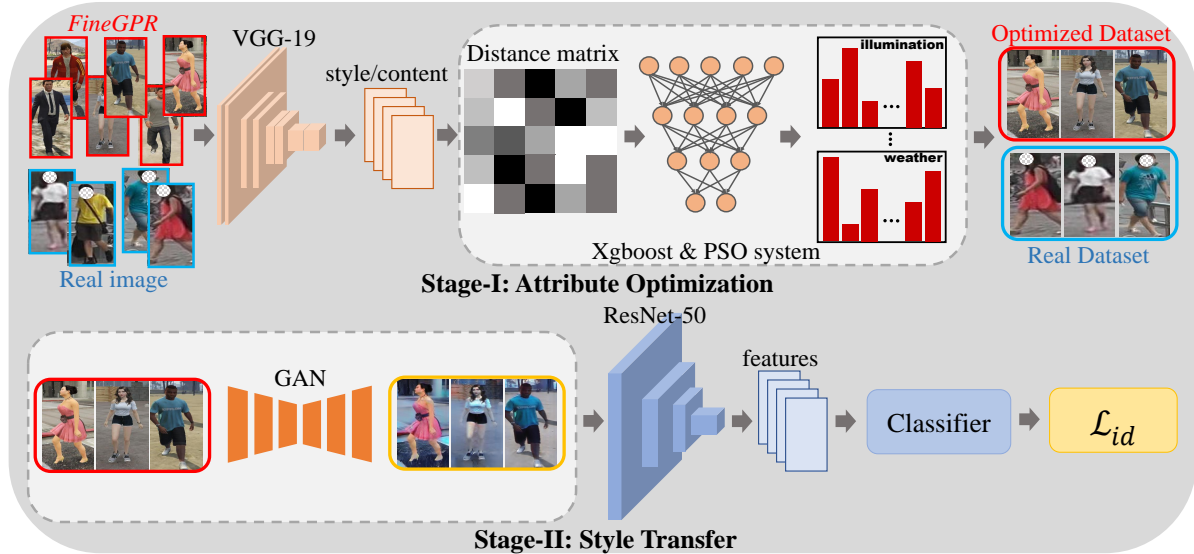


Figure 4. The two-stage pipeline AOST to learn attribute distribution of target domain. Firstly, we learn attribute distribution of real domain on the basis of XGBoost & PSO learning system. Secondly, we perform style transfer to enhance the reality of optimal dataset. Finally, the transferred data are adopted for downstream re-ID task.



Figure 5. Some visual examples of collected MSCO dataset.

and $\mathcal{D}_{\text{total}}$. Based on the upgraded Xgboost model θ^* , we continuously adopt a widely used Particle Swarm Optimization (PSO) [19] method to search some optimized attributes. Typically, it selects a similar style or content distribution with respect to a real target dataset. The optimization framework can be shown in Fig. 4 (Stage I). To our knowledge this is the first demonstration to perform attribute optimization with large-scale synthetic dataset on person re-ID task. In essence, compared with existing methods for attribute optimization, such as reinforcement learning [29] and attribute descent [42], our method investigates and learns these attribute distributions only with few parameters to optimize, which makes it more flexible and adaptable.

Style Transfer. In the above attribute optimization stage, there exists serious domain gap or distribution shift between synthetic and real-world scenario. Generative Adversarial Networks (GAN) [14] which have demonstrated impressive results on image-to-image translation seem to be a natural solution to this problem. However, existing methods are both inefficient and ineffective in practical application. Their inefficiency results from the fact that a new generator needs to be retrained when given a new real-world scenario. Meanwhile, these methods mainly employ low-resolution

Algorithm 1 The Proposed AOST Method

Input: Labeled synthetic data L ; Unlabeled real target data U ;
 Initialized VGG model ϕ ; Xgboost model θ_0 ;
 Two hyper-parameters α and β ; Iteration rounds n ;
Output: Best re-ID model $f(w, x_i)$

- 1: Initialize: $m = 1, \text{iter} = 1$;
- 2: \triangleright *Attribute Optimization* ***
- 3: Extract $\mathcal{D}_{\text{style}}$ & $\mathcal{D}_{\text{content}}$ between L and U with model ϕ ;
- 4: $\mathcal{D}_{\text{total}} \leftarrow \alpha * \mathcal{D}_{\text{style}} + \beta * \mathcal{D}_{\text{content}}$;
- 5: **while** $m \leq \|U\|$ **do**
- 6: Optimized model $\theta^* \leftarrow$ train θ_0 with L and $\mathcal{D}_{\text{total}}$;
- 7: Optimized attributes $\mathcal{V}^* \leftarrow$ update θ^* with PSO;
- 8: Update the sample size: $m \leftarrow m + 1$;
- 9: **end while**
- 10: Generate a new dataset L^* according to \mathcal{V}^* ;
- 11: \triangleright *Style Transfer* ***
- 12: Performing style transfer with GAN on L^* ;
- 13: **if** $\text{iter} \leq n$ **then**
- 14: Initializing re-ID model with L^* by softmax loss ;
- 15: $\text{iter} \leftarrow \text{iter} + 1$;
- 16: **end if**

images to train a generator, and they are incapable of fully exploiting the potential of GAN, which is likely to limit the quality of generated images. To provide a remedy to this dilemma, we build a high-resolution dataset MSCO and crawled over 20K images with a size of nearly 200×480 , which mainly from COCO [24] dataset and few from other real-world person datasets. Different locations are also considered to cover a large diversity. We believe that a unified dataset with high-resolution can provide more useful and

Testing set →			Market-1501			MSMT17			CUHK03		
Training set ↓	Reference	Synthetic data	Rank-1	Rank-5	mAP	Rank-1	Rank-5	mAP	Rank-1	Rank-5	mAP
Market-1501 [46]	ICCV 15	×	<u>92.7</u>	<u>97.9</u>	<u>81.4</u>	6.0	11.2	1.9	5.3	12.4	6.2
MSMT17 [39]	CVPR 18	×	50.2	67.7	25.7	<u>75.7</u>	<u>86.9</u>	<u>51.5</u>	9.9	20.4	10.7
CUHK03 [21]	CVPR 14	×	36.6	53.9	16.6	4.6	9.1	1.3	<u>43.6</u>	<u>62.9</u>	<u>41.5</u>
SOMAsen* [2]	CVIU 18	✓	4.5	–	1.3	1.4	–	0.3	0.4	–	0.4
SyRI* [1]	ECCV 18	✓	29.0	–	10.8	16.4	–	4.4	4.1	–	3.5
Unreal [‡] [43]	CVPR 21	✓	37.4	55.2	15.9	3.9	7.4	1.3	4.3	10.0	4.7
PersonX* [32]	CVPR 19	✓	44.0	–	20.4	11.7	–	3.6	7.4	–	6.2
RandPerson* [38]	MM 20	✓	55.6	–	28.8	20.1	–	6.3	13.4	–	10.8
<i>FineGPR</i>	Ours	✓	50.5	67.7	24.6	12.5	18.5	3.9	8.7	18.2	8.4
<i>FineGPR</i> [†]	Ours	✓	56.3	70.4	29.2	19.7	27.4	6.1	14.2	20.6	11.2

Table 2. Performance comparison with existing Real and Synthetic datasets on Market-1501, MSMT17 and CUHK03, respectively. **Red** indicates the best and **Blue** the second best. * means results are reported by RandPerson [38]. ‡ represents results reproduced with Unreal_v2.1 on our baseline. Underline denotes supervised learning. † means performing selecting with our AOST method.

discriminative information during translation. Some visual examples of collected MSCO dataset are illustrated in Fig 5. By doing so, we only need to train one generator and translate the synthetic images into photo-realistic style at testing phase. The details can be seen in Fig. 4 (**Stage II**). To verify the priority of MSCO, we adopt several state-of-the-art methods for style-level domain adaptation, e.g., CycleGAN [49], PTGAN [39] and SPGAN [9].

5. Experiments

5.1. Datasets and Evaluation

Market-1501 [46] contains 32,668 labeled images of 1,501 identities captured from campus in Tsinghua University. Each identity is captured by at most 6 cameras. The training set contains 12,936 images from 751 identities and the test set contains 19,732 images from 750 identities.

MSMT17 [39] has 126,441 labeled images belonging to 4,101 identities and contains 32,621 training images from 1,041 identities. For the testing set, 11,659 bounding boxes are used as query images and other 82,161 bounding boxes are used as gallery images.

CUHK03 [21] contains 14,097 images of 1,467 identities. Following the CUHK03-NP protocol [48], it is divided into 7,365 images of 767 identities as the training set, and the remaining 6,732 images of 700 identities as the testing set. We adopt mean Average Precision (mAP) and Cumulative Matching Characteristics (CMC) at rank-1 and rank-5 for evaluation on re-ID task.

5.2. Experiment Settings

We mainly use the newly-built *FineGPR* to conduct the experiments. For attribute optimization, we empirically set $w_l = 0.2$ in Eq. 2, and $\alpha = 0.9$, $\beta = 1$ in Eq. 3. It is worth mentioning that our re-ID baseline system is built only with commonly used softmax cross-entropy loss [44] on vanilla ResNet-50 [16] with no bells and whistles. Following the

practice in [25], person images are resized to 256×128 , then a random horizontal flipping with 0.5 probability is used for data augmentation. The batch size of training samples is set as 128. Adam method [20] is adopted for optimization. The initial learning rate is set to 3.5×10^{-4} for the backbone network. Then, these learning rates are decayed to 3.5×10^{-5} and 3.5×10^{-6} at 40th epoch and 70th epoch respectively, and the training stops after 120 epochs.

5.3. Comparison with the State-of-the-arts

To evaluate the superiority of our synthetic dataset, we perform training on *FineGPR* and testing on each individual real dataset. The evaluation results are reported in Table 2. Surprisingly, when initializing with whole *FineGPR* dataset, we can achieve a rank-1 accuracy of **50.5%**, **12.5%** and **8.7%** when tested on Market-1501, MSMT17 and CUHK03 respectively. Although there is a slight inferiority of performance when compared with RandPerson [38], our *FineGPR* selected by AOST with fine-grained attributes can lead a significant improvement by **+0.7%** and **+0.8%** in rank-1 accuracy on Market-1501 and CUHK03 dataset respectively. When compared with real-world datasets, *FineGPR* also outperforms these benchmarks by an impressively large margin in terms of rank-1 accuracy, leading **+0.3%** and **+13.9%** improvement on Market-1501 compared with MSMT17 and CUHK03 separately. However, initializing with whole *FineGPR* dataset is time-consuming and low-efficient, this motivates the investigation of data selecting techniques that can potentially address this problem.

5.4. Ablation Study

Important Parameters. In Eq. 3, both α and β controls the relative importance of the style and content distance respectively between real and synthetic samples. Since $\mathcal{D}_{\text{total}}$ is a linear combination between $\mathcal{D}_{\text{style}}$ and $\mathcal{D}_{\text{content}}$, we can smoothly regulate the emphasis or adjust the trade-off between the content or the style. As depicted in Fig. 6 (a),

Testing set →			Market-1501			MSMT17			CUHK03		
Training set ↓	Bboxes	Time (GPU-days) ↓	Rank-1	Rank-5	mAP	Rank-1	Rank-5	mAP	Rank-1	Rank-5	mAP
<i>FineGPR</i>	2,028,600	20	50.5	67.7	24.6	12.5	18.5	3.9	8.7	18.2	8.4
<i>FineGPR</i> +R	124,200	1.3	39.9	57.1	18.3	4.6	9.7	1.4	5.9	15.4	5.4
<i>FineGPR</i> +AO (w/o transfer)	124,200	1.3	45.5	63.2	23.8	9.1	14.7	3.1	8.5	16.9	8.3
PersonX+R+ST	124,200	1.3	28.7	45.9	11.8	7.1	13.4	2.1	3.1	7.4	3.1
Unreal+R+ST	124,200	1.3	42.8	59.3	18.4	11.3	20.5	3.5	5.4	12.6	5.1
RandPerson+R+ST	124,200	1.3	51.4	68.3	25.0	15.8	26.7	5.0	8.4	18.1	7.5
<i>FineGPR</i> +AOST (Ours)	124,200	1.3	56.3	70.4	29.2	19.7	27.4	6.1	14.2	20.6	11.2

Table 3. Controlled experiments by different regulations of our proposed AOST method on Market-1501, MSMT17 and CUHK03, respectively. “R” indicates random sampling, “AO” represents Attribute Optimization. “ST” means Style Transfer.

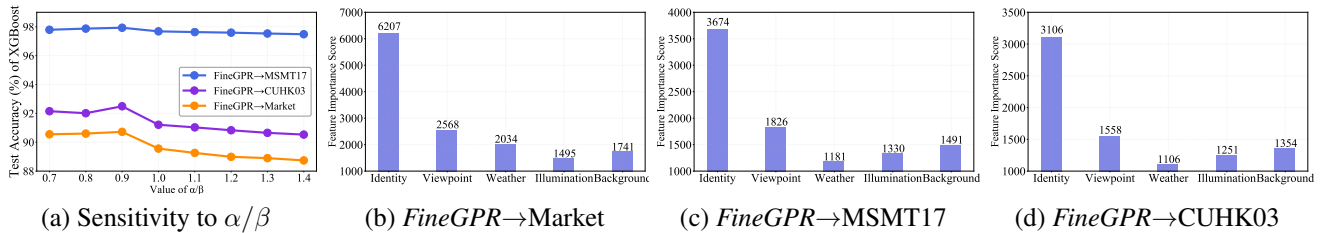


Figure 6. (a) Sensitivity of AOST to key parameter α/β in Eq. 3. (b-d) Feature importance of XGBoost with Feature Importance Score (higher is more important) on Market-1501, MSMT17 and CUHK03 respectively. Please zoom in for the best view.

we observe that when α/β is small, the performances is not optimal because the style representation is way too limited to a very small portion, and thus our AOST could only mine the discriminative information in terms of content representation of the re-ID data. The α/β should also not be set too large, otherwise the performances drops dramatically since the model mine too many samples in style representation. Specially, $\alpha/\beta = 0.9$ yields the best accuracy.

Evaluation of Attribute Importance. Based on the end-to-end AOST system, we evaluate the impacts of different attributes in a fine-grained manner by the XGBoost in terms of *gain* [4] (feature importance score). As illustrated in Fig. 6 (b-d), it can be easily observed that **Identity** accounts for the largest proportion no matter which real dataset is employed for testing, followed by **Viewpoint** attribute. Typically, this conclusion is in accordance with our prior knowledge on generalizable re-ID problem, that is, *using more IDs as training samples is always beneficial to the re-ID system, and viewpoint also plays a key role in recognizing the clothes appearance*. More details about the importance related to ID-level attributes is provided in the Supplementary. We hope these analysis about attribute importance will provide useful insights for dataset building and future practical usage to the community.

Effectiveness of Attribute Optimization. We proceed study on dependency by testing whether the Attribute Optimization (AO) matters. According to Table 3, our attribute optimization strategy *FineGPR*+AO (w/o

transfer) can lead a significant improvement in rank-1 of **+5.6%**, **+4.5%** and **+2.6%** on Market-1501, MSMT17 and CUHK03 respectively when compared with random sampling (*FineGPR*+R). We suspect this is due to samples selected by attribute optimization strategy are much closer to real target domain, and the learned attribute distribution has a higher quality, which have a direct impact on downstream re-ID task. Meanwhile, fast training is our second main advantage since the scale of training set can be largely decreased by attribute optimization, *e.g.*, it costs nearly 20 GPU-days¹ when pre-training on entire *FineGPR* with 2,028,600 images. Fortunately, training time will be considerably reduced by **15×** (20 vs. 1.3 GPU-days) by our proposed AOST without performance degradation, which leads a more efficient deployment to real-world scenarios. Surprisingly, even with fewer samples for training, our approach still yields its competitiveness when compared with existing datasets, *e.g.* **56.3%** vs. **55.6%** in rank-1 on Market in Table 2, proving the proverbial *less-is-more* principle.

To go even further, we also adopt AOST on synthetic datasets to prove the priority of *FineGPR*. Unfortunately, due to lack of fine-grained attribute annotations, these datasets (*e.g.* PersonX, Unreal and RandPerson) cannot satisfy the need for AOST in re-ID. We instead randomly sample 124,200 images from these datasets individually, and then perform style transfer. As illustrated in Table 3, it can

¹All timings use one Nvidia Tesla P100 GPU on a server equipped with an Intel Xeon E5-2690 V4 CPU.



Figure 7. Qualitative comparisons of different GAN methods when trained on Market and our MSCO, respectively.

be easily observed that *FineGPR*+AOST can perform significantly greater than PersonX+R+ST, Unreal+R+ST and RandPerson+R+ST separately, which successfully proves the applicability of our proposed dataset and approach.

Effectiveness of Style Transfer. Synthetic data engine can generate images and annotations at lower labor costs. However, there exists obvious domain gap between synthetic and real-world scenario, which hinders the further improvement in performance on downstream task. Note that for training efficiency, we instead consider an easier but practical strategy, that is, employing off-the-shelf style transfer model to generate photo-realistic images for further effective training. As shown in Table 3, *w/o* style transfer by AOST, the rank-1 accuracy drops sharply from 56.3% to 45.5% and the mAP drops from 29.2% to 23.8%. *This confirms that mitigating domain gap between synthetic and real dataset is a crucial ingredient to make the performance to an excellent level.* For simplicity, the SPGAN is used as the style transfer model in the following experiments.

5.5. Qualitative and Quantitative Results

Qualitative Evaluations. Fig. 7 presents a visual comparison of different transfer methods trained on low-resolution Market and high-resolution MSCO respectively. It can be easily noticed that GANs create artifacts and coarse results (indicated by yellow box) when trained on low-resolution images, which still remains problematic. In comparison, our method with MSCO can successfully address the artifacts and produce most visually pleasant results (indicated by red box) in an even better fashion, which is implicitly beneficial to the downstream re-ID mission.

Quantitative Evaluations. Our qualitative observations above are confirmed by the quantitative evaluations. To be more specific, we adopt Fréchet Inception Distance (FID) [18] to measure the distribution difference between synthetic and real photos. Generally, FID measures how close the distribution of generated images is to the real. As shown in Fig. 8, by adding new regulation terms, *e.g.* at-

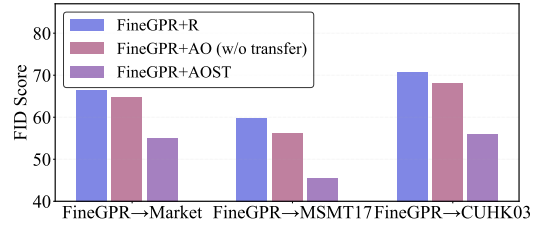


Figure 8. Comparison of FID (lower is better) to evaluate the effectiveness of different regulation terms of AOST.

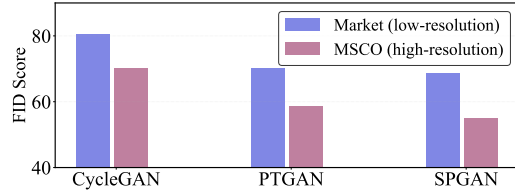


Figure 9. Comparison of FID (lower is better) to evaluate the realism of generated images by CycleGAN, PTGAN and SPGAN when trained on samples with different resolution.

tribute optimization or style transfer, the FID score gradually decreases no matter which dataset is employed for evaluation, suggesting the learned attribute distributions are more and more similar to the real images. Even prior to this point, according to Fig. 9, training a generator with low-resolution images always produce low-quality images (indicated by higher FID score) no matter which style transfer model is employed. Still, SPGAN and PTGAN rank the best, while SPGAN shows a slight quantitative advantage. In all, the introduction of high-resolution MSCO dataset can always improve the adaptability to style changes and mitigate previously mentioned domain gap effectively, even in much more complex scenarios.

6. Conclusion

In this work, we take the first step to construct the largest person dataset *FineGPR* with fine-grained attribute labels and high-quality annotations. On top of *FineGPR*, we introduce an attribute analysis methodology called AOST to learn important attribute distribution, which enjoys the benefits of small-scale dataset for more efficient training. Continuously, style transfer is adopted to further mitigate domain gap between synthetic and real photos. With this, we proved, for the first time, that a model trained on limited synthetic data can yield a competitive performance in generalizable re-ID task. Extensive experiments also demonstrate the superiority of *FineGPR* and effectiveness of AOST. We hope our dataset and method will shed light into potential tasks for the community to move forward.

References

- [1] Slawomir Bak, Peter Carr, and Jean-Francois Lalonde. Domain adaptation through synthesis for unsupervised person re-identification. In *Proceedings of the European Conference on Computer Vision (ECCV)*, pages 189–205, 2018. 1, 2, 3, 6
- [2] Igor Barros Barbosa, Marco Cristani, Barbara Caputo, Alexander Rognhaugen, and Theoharis Theoharis. Looking beyond appearances: Synthetic training data for deep cnns in re-identification. *Computer Vision and Image Understanding*, 167:50–62, 2018. 1, 3, 6
- [3] Joy Buolamwini and Timnit Gebru. Gender shades: Intersectional accuracy disparities in commercial gender classification. In *Conference on fairness, accountability and transparency*, pages 77–91. PMLR, 2018. 4
- [4] Tianqi Chen and Carlos Guestrin. Xgboost: A scalable tree boosting system. In *Proceedings of the 22nd acm sigkdd international conference on knowledge discovery and data mining*, pages 785–794, 2016. 4, 7
- [5] Weihua Chen, Xiaotang Chen, Jianguo Zhang, and Kaiqi Huang. Beyond triplet loss: a deep quadruplet network for person re-identification. In *Proceedings of the IEEE conference on computer vision and pattern recognition*, pages 403–412, 2017. 2
- [6] Yuhua Chen, Wen Li, Xiaoran Chen, and Luc Van Gool. Learning semantic segmentation from synthetic data: A geometrically guided input-output adaptation approach. In *Proceedings of the IEEE/CVF Conference on Computer Vision and Pattern Recognition*, pages 1841–1850, 2019. 3
- [7] Abir Das, Anirban Chakraborty, and Amit K Roy-Chowdhury. Consistent re-identification in a camera network. In *European conference on computer vision*, pages 330–345. Springer, 2014. 3
- [8] Jia Deng, Wei Dong, Richard Socher, Li-Jia Li, Kai Li, and Li Fei-Fei. Imagenet: A large-scale hierarchical image database. In *2009 IEEE conference on computer vision and pattern recognition*, pages 248–255. Ieee, 2009. 4
- [9] Weijian Deng, Liang Zheng, Qixiang Ye, Guoliang Kang, Yi Yang, and Jianbin Jiao. Image-image domain adaptation with preserved self-similarity and domain-dissimilarity for person re-identification. In *Proceedings of the IEEE conference on computer vision and pattern recognition*, pages 994–1003, 2018. 2, 6
- [10] Matteo Fabbri, Guillem Brasó, Gianluca Maueri, Orcun Cetintas, Riccardo Gasparini, Aljosa Osep, Simone Calderara, Laura Leal-Taixe, and Rita Cucchiara. Motsynth: How can synthetic data help pedestrian detection and tracking? In *Proceedings of the IEEE/CVF International Conference on Computer Vision*, pages 10849–10859, 2021. 4
- [11] Yaroslav Ganin and Victor Lempitsky. Unsupervised domain adaptation by backpropagation. In *International conference on machine learning*, pages 1180–1189. PMLR, 2015. 2
- [12] Leon A Gatys, Alexander S Ecker, and Matthias Bethge. Image style transfer using convolutional neural networks. In *Proceedings of the IEEE conference on computer vision and pattern recognition*, pages 2414–2423, 2016. 4
- [13] Michelle Goddard. The eu general data protection regulation (gdpr): European regulation that has a global impact. *International Journal of Market Research*, 59(6):703–705, 2017. 1
- [14] Ian Goodfellow, Jean Pouget-Abadie, Mehdi Mirza, Bing Xu, David Warde-Farley, Sherjil Ozair, Aaron Courville, and Yoshua Bengio. Generative adversarial nets. *Advances in neural information processing systems*, 27, 2014. 5
- [15] Douglas Gray, Shane Brennan, and Hai Tao. Evaluating appearance models for recognition, reacquisition, and tracking. In *Proc. IEEE international workshop on performance evaluation for tracking and surveillance (PETS)*, volume 3, pages 1–7. Citeseer, 2007. 3
- [16] Kaiming He, Xiangyu Zhang, Shaoqing Ren, and Jian Sun. Deep residual learning for image recognition. In *Proceedings of the IEEE conference on computer vision and pattern recognition*, pages 770–778, 2016. 1, 6
- [17] Alexander Hermans, Lucas Beyer, and Bastian Leibe. In defense of the triplet loss for person re-identification. *arXiv preprint arXiv:1703.07737*, 2017. 2
- [18] Martin Heusel, Hubert Ramsauer, Thomas Unterthiner, Bernhard Nessler, and Sepp Hochreiter. Gans trained by a two time-scale update rule converge to a local nash equilibrium. *Advances in neural information processing systems*, 30, 2017. 8
- [19] James Kennedy and Russell Eberhart. Particle swarm optimization. In *Proceedings of ICNN'95-international conference on neural networks*, volume 4, pages 1942–1948. IEEE, 1995. 5
- [20] Diederik P Kingma and Jimmy Ba. Adam: A method for stochastic optimization. *arXiv preprint arXiv:1412.6980*, 2014. 6
- [21] Wei Li, Rui Zhao, Tong Xiao, and Xiaogang Wang. Deepreid: Deep filter pairing neural network for person re-identification. In *Proceedings of the IEEE conference on computer vision and pattern recognition*, pages 152–159, 2014. 2, 3, 6
- [22] Wei Li, Xiatian Zhu, and Shaogang Gong. Harmonious attention network for person re-identification. In *Proceedings of the IEEE conference on computer vision and pattern recognition*, pages 2285–2294, 2018. 2
- [23] Shengcai Liao, Yang Hu, Xiangyu Zhu, and Stan Z Li. Person re-identification by local maximal occurrence representation and metric learning. In *Proceedings of the IEEE conference on computer vision and pattern recognition*, pages 2197–2206, 2015. 2
- [24] Tsung-Yi Lin, Michael Maire, Serge Belongie, James Hays, Pietro Perona, Deva Ramanan, Piotr Dollár, and C Lawrence Zitnick. Microsoft coco: Common objects in context. In *European conference on computer vision*, pages 740–755. Springer, 2014. 5
- [25] Hao Luo, Youzhi Gu, Xingyu Liao, Shenqi Lai, and Wei Jiang. Bag of tricks and a strong baseline for deep person re-identification. In *Proceedings of the IEEE/CVF Conference on Computer Vision and Pattern Recognition Workshops*, pages 0–0, 2019. 2, 6
- [26] Xingang Pan, Ping Luo, Jianping Shi, and Xiaoou Tang. Two at once: Enhancing learning and generalization capacities

- via ibn-net. In *Proceedings of the European Conference on Computer Vision (ECCV)*, pages 464–479, 2018. 1
- [27] Bojan Pepik, Michael Stark, Peter Gehler, and Bernt Schiele. Teaching 3d geometry to deformable part models. In *2012 IEEE conference on computer vision and pattern recognition*, pages 3362–3369. IEEE, 2012. 3
- [28] Ergys Ristani, Francesco Solera, Roger Zou, Rita Cucchiara, and Carlo Tomasi. Performance measures and a data set for multi-target, multi-camera tracking. In *European conference on computer vision*, pages 17–35. Springer, 2016. 1
- [29] Nataniel Ruiz, Samuel Schulter, and Manmohan Chandraker. Learning to simulate. *arXiv preprint arXiv:1810.02513*, 2018. 5
- [30] William Robson Schwartz and Larry S Davis. Learning discriminative appearance-based models using partial least squares. In *2009 XXII Brazilian symposium on computer graphics and image processing*, pages 322–329. IEEE, 2009. 3
- [31] Karen Simonyan and Andrew Zisserman. Very deep convolutional networks for large-scale image recognition. *arXiv preprint arXiv:1409.1556*, 2014. 4
- [32] Xiaoxiao Sun and Liang Zheng. Dissecting person re-identification from the viewpoint of viewpoint. In *Proceedings of the IEEE/CVF Conference on Computer Vision and Pattern Recognition*, pages 608–617, 2019. 1, 3, 6
- [33] Antonio Torralba and Alexei A Efros. Unbiased look at dataset bias. In *CVPR 2011*, pages 1521–1528. IEEE, 2011. 2
- [34] Rahul Rama Vavior, Mrinal Haloi, and Gang Wang. Gated siamese convolutional neural network architecture for human re-identification. In *European conference on computer vision*, pages 791–808. Springer, 2016. 2
- [35] Rahul Rama Vavior, Bing Shuai, Jiwen Lu, Dong Xu, and Gang Wang. A siamese long short-term memory architecture for human re-identification. In *European conference on computer vision*, pages 135–153. Springer, 2016. 2
- [36] Faqiang Wang, Wangmeng Zuo, Liang Lin, David Zhang, and Lei Zhang. Joint learning of single-image and cross-image representations for person re-identification. In *Proceedings of the IEEE Conference on Computer Vision and Pattern Recognition*, pages 1288–1296, 2016. 2
- [37] Qi Wang, Junyu Gao, Wei Lin, and Yuan Yuan. Learning from synthetic data for crowd counting in the wild. In *Proceedings of the IEEE/CVF Conference on Computer Vision and Pattern Recognition*, pages 8198–8207, 2019. 3
- [38] Yanan Wang, Shengcai Liao, and Ling Shao. Surpassing real-world source training data: Random 3d characters for generalizable person re-identification. In *Proceedings of the 28th ACM International Conference on Multimedia*, pages 3422–3430, 2020. 1, 2, 3, 6
- [39] Longhui Wei, Shiliang Zhang, Wen Gao, and Qi Tian. Person transfer gan to bridge domain gap for person re-identification. In *Proceedings of the IEEE conference on computer vision and pattern recognition*, pages 79–88, 2018. 3, 6
- [40] Suncheng Xiang, Yuzhuo Fu, Guanjie You, and Ting Liu. Unsupervised domain adaptation through synthesis for person re-identification. In *2020 IEEE International Conference on Multimedia and Expo (ICME)*, pages 1–6. IEEE, 2020. 2
- [41] Tong Xiao, Shuang Li, Bochao Wang, Liang Lin, and Xiaogang Wang. Joint detection and identification feature learning for person search. In *Proceedings of the IEEE Conference on Computer Vision and Pattern Recognition*, pages 3415–3424, 2017. 2
- [42] Yue Yao, Liang Zheng, Xiaodong Yang, Milind Naphade, and Tom Gedeon. Simulating content consistent vehicle datasets with attribute descent. In *Computer Vision—ECCV 2020: 16th European Conference, Glasgow, UK, August 23–28, 2020, Proceedings, Part VI 16*, pages 775–791. Springer, 2020. 5
- [43] Tianyu Zhang, Lingxi Xie, Longhui Wei, Zijie Zhuang, Yongfei Zhang, Bo Li, and Qi Tian. Unrealperson: An adaptive pipeline towards costless person re-identification. In *Proceedings of the IEEE/CVF Conference on Computer Vision and Pattern Recognition*, pages 11506–11515, 2021. 3, 6
- [44] Zhilu Zhang and Mert R Sabuncu. Generalized cross entropy loss for training deep neural networks with noisy labels. In *32nd Conference on Neural Information Processing Systems (NeurIPS)*, 2018. 6
- [45] Rui Zhao, Wanli Ouyang, and Xiaogang Wang. Learning mid-level filters for person re-identification. In *Proceedings of the IEEE conference on computer vision and pattern recognition*, pages 144–151, 2014. 2
- [46] Liang Zheng, Liyue Shen, Lu Tian, Shengjin Wang, Jingdong Wang, and Qi Tian. Scalable person re-identification: A benchmark. In *Proceedings of the IEEE international conference on computer vision*, pages 1116–1124, 2015. 1, 2, 3, 6
- [47] Zhedong Zheng, Liang Zheng, and Yi Yang. Unlabeled samples generated by gan improve the person re-identification baseline in vitro. In *Proceedings of the IEEE international conference on computer vision*, pages 3754–3762, 2017. 1
- [48] Zhun Zhong, Liang Zheng, Donglin Cao, and Shaozi Li. Re-ranking person re-identification with k-reciprocal encoding. In *Proceedings of the IEEE conference on computer vision and pattern recognition*, pages 1318–1327, 2017. 6
- [49] Jun-Yan Zhu, Taesung Park, Phillip Isola, and Alexei A Efros. Unpaired image-to-image translation using cycle-consistent adversarial networks. In *Proceedings of the IEEE international conference on computer vision*, pages 2223–2232, 2017. 6